Multimodel Ensemble Reconstruction of Drought over the Continental United States

AIHUI WANG* AND THEODORE J. BOHN

Department of Civil and Environmental Engineering, University of Washington, Seattle, Washington

SARITH P. MAHANAMA AND RANDAL D. KOSTER

Global Modeling and Assimilation Office, NASA Goddard Space Flight Center, Greenbelt, Maryland

DENNIS P. LETTENMAIER

Department of Civil and Environmental Engineering, University of Washington, Seattle, Washington

(Manuscript received 15 April 2008, in final form 8 September 2008)

ABSTRACT

Retrospectively simulated soil moisture from an ensemble of six land surface/hydrological models was used to reconstruct drought events over the continental United States for the period 1920–2003. The simulations were performed at one-half-degree spatial resolution, using a common set of atmospheric forcing data and model-specific soil and vegetation parameters. Monthly simulated soil moisture was converted to percentiles using Weibull plotting position statistics, and the percentiles were then used to represent drought severities and durations. An ensemble method, based on an inverse mapping of the average of the individual model's soil moisture percentiles, was also used to combine all models' simulations. Major results are 1) all models and the ensemble reconstruct the known severe drought events during the last century. The spatial extents and severities of drought are plausible for the individual models although substantial among-model disparities exist. 2) The simulations are in more agreement with each other over the eastern than over the western United States. 3) Most of the models show that soil moisture memory is much longer over the western than over the eastern United States. The results provide some insights into how a hydrological nowcast system can be developed, and also early results from a test application within the University of Washington's real-time national Surface Water Monitor and a review of the multimodel nowcasts during the southeastern drought beginning in summer 2007 are included.

1. Introduction

Droughts are a recurrent and costly natural hazard. According to a report of the Martz et al. (2003), an ''extreme'' or ''severe'' drought has been experienced in some part of the United States in every year since 1895. The 1988 drought alone cost nearly $62 billion, more than the cost of the 1993 Mississippi River flood and Hurricane Andrew combined (Ross and Lott 2003). Historically, droughts of decadal length or longer, such as the Dust Bowl drought of the 1930s, have occurred 1 or 2 times per century on average (Woodhouse and Overpeck 1998). Globally, the areal extent of droughts increased more than 50% during last century, while changes in areal extent of wet regions were relatively small (Trenberth 2004). Trenberth et al. (2007) reviewed the evidence of drought in North America and found that the southwestern United States, northwestern Mexico, and the Baja Peninsula in Mexico are particularly susceptible to drought.

A number of recent studies have suggested that the interior of the Northern Hemisphere continents will become more susceptible to droughts over the next century as a result of greenhouse warming. Dai et al. (2004) concluded that anthropogenic global warming induces an increasing risk of drought based on an analysis of reconstructed historical Palmer drought severity index data (PDSI). On the other hand, Andreadis

* Current affiliation: Institute of Atmospheric Physics, Chinese Academy of Sciences, Beijing, China.

Corresponding author address: Dennis P. Lettenmaier, Department of Civil and Environmental Engineering, 164 Wilcox Hall, Box 352700, Seattle, WA 98195-2700.
E-mail: dennisl@u.washington.edu

DOI: 10.1175/2008JCLI2586.1

© 2009 American Meteorological Society

and Lettenmaier (2006) found that, over much of the continental United States, droughts became less severe as a result of wetter conditions over the last 80 yr; however, there was some indication of increased drought severity over the western United States where increased evaporative demand seemed to have countered increased precipitation to result in reduced soil moisture.

Droughts can be classified according to their characteristics and impacts as falling in one of four categories: agricultural, meteorological, hydrological, and socioeconomic (AMS Council 1997); however, most droughts are classified, based on their physical characteristics, into one of the first three categories. Two methods have been used to assess and reconstruct past droughts. The first is based on indexes derived from meteorological and hydrological data. The most prominent drought index is the PDSI (Palmer 1965), which is driven by precipitation and temperature but essentially reconstructs a soil moisture index. This index has been extensively used in drought studies (e.g., Karl 1983, 1986). Dai et al. (2004) reconstructed PDSI for the entire global land area based on historical precipitation and temperature data. They found a close relationship between monthly PDSI and monthly soil moisture in warm season months and between basin-averaged annual PDSI and streamflow over large river basins. They also found that PDSI is poorly correlated with soil moisture in cold seasons because of the influence of snowmelt. Alley (1984) summarized limitations of PDSI, such as arbitrary criteria for determination of drought properties (e.g., intensity and timing) and absence of a basis for interpreting the values at different locations. Other popular drought indexes include the standardized precipitation index (SPI) and the surface water supply index (Keyantash and Dracup 2002). These indexes are indirectly linked to long-term time series of observations.

Another method of assessing drought severity is to analyze simulated variables from atmospheric or hydrological models. The major advantage of this approach is that it is based on variables (soil moisture, runoff) that are directly related to drought properties. A further advantage of this approach is a direct link (i.e., by providing model initial conditions) to predictions of future droughts. One example of this approach, based on a (global) coupled land–atmosphere model, is the study of North American drought by Schubert et al. (2004a). They found, using an atmosphere general circulation model (AGCM) forced with observed SSTs, that drought over the Great Plains is linked to abnormal tropical Pacific SSTs. They also found that soil moisture feedback increases the variance of simulated precipitation, to which both agricultural and meteorological drought are related.

A drawback of using coupled land–atmosphere models to reproduce drought-related variables is that they are reliant on the accuracy of the parameterizations and land–atmosphere feedback mechanisms incorporated in the model—for instance, model errors in cloud and radiation parameterizations affect both precipitation and evapotranspiration. An alternative approach is to use land surface models (LSMs) offline (i.e., forced by surface meteorological variables such as precipitation, temperature, and downward shortwave and longwave radiation), an approach that removes the effects of atmospheric model errors. The drought-related variables so produced can provide insights into possible characteristics, and perhaps mechanisms, of future drought. Andreadis et al. (2005) used this approach to reconstruct agricultural and hydrologic drought over the conterminous United States for the period 1920–2003 with the Variable Infiltration Capacity (VIC; Liang et al. 1994) macroscale hydrological model. They were able to reconstruct the major drought events of the twentieth century over the continental United States, including those of the 1930s and mid-1950s. They also developed a method, which they termed severity–area–duration (SAD) analysis, to characterize relationships among drought severity, area covered, and duration. SAD is an adaptation of the widely used depth–area–duration (DAD) method for design storm analysis (World Meteorological Organization 1969).

The U.S. Drought Monitor (Svoboda et al. 2002) uses a combination of the above two methods to fuse climate indexes (such as PDSI), and the outputs of numerical models, as well as input from regional and local experts into maps of current drought extent.

This product is not a forecast tool, but rather an assessment of current drought conditions. While the Drought Monitor provides a useful reference for socioeconomic and agricultural management purposes, there is a concern that its estimates of drought extent, and changes in drought extent, are not reproducible in an objective manner.

The use of macroscale hydrological models, driven by observed meteorological data, resolves this concern. This approach has been used for several years in the experimental University of Washington West-Wide Hydrological Forecast System (Wood and Lettenmaier 2006). However, the west-wide forecast system (and companion U.S. surface water monitor, see http://www.hydro.washington.edu/forecast/monitor) is based on a single LSM and therefore does not represent variations in drought delineations that may result from use of alternative LSMs. In this paper, we implement and evaluate a suite of multiple LSMs over the continental United States and apply the SAD procedure outlined in Andreadis et al.

TABLE 1. Comparison of major features of model structures and hydrological schemes.

Model	Soil hydrology scheme	Soil layers and depth	Soil/vegetation parameters	References
VIC	Variable infiltration capacity curve for surface runoff, ARNO model for base flow, and drainage driven by gravity	3 soil layers with depths specified differently cell by cell. Total depth ranges from 0.8 to 3 m	From NLDAS	Liang et al. (1994), Maurer et al. (2002), Mitchell et al. (2004)
CLM3.5	TOPMODEL-based surface runoff; groundwater scheme	10 soil layers and fixed depth. Total soil depth is 3.43 m	Vegetation data are from Moderate Resolution Imaging Spectroradiometer (MODIS), and soil data are from International Geosphere-Biosphere Programme (IGBP) dataset	Bonan et al. (2002), Oleson et al. (2007), Niu et al. (2005, 2007)
Noah	Exponential distribution of infiltration capacity for runoff; base flow proportional to storage; drainage driven by gravity	4 soil layers and fixed depth. Total soil depth is 2 m	Soil and vegetation parameters from NLDAS	Schaake et al. (1996), Chen et al. (1997), Koren et al. (1999), Ek et al. (2003), Mitchell et al. (2004)
Sac	Runoff from impervious and saturated soils; base flow and percolation between reservoirs based on current storage	5 soil water storage reservoirs. Total storage capacity ranges from 20 to 600 mm	No vegetation; soil parameters from NLDAS	Burnash et al. (1973), Anderson (1973), Mitchell et al. (2004)
Catchment	TOPMODEL-based soil hydrology scheme	Total soil depth is from 1.0 to 1.52 m	Soil depth from State Soil Geographic Database (STATSGO); soil texture from the Food and Agriculture Organization (FAO); vegetation classification from IGBP; soil and vegetation parameters are consistent with Global Soil Wetness Project (GSWP)-2 global parameters	Koster et al. (2000a), Ducharne et al. (2000)
CLM–VIC	Same as VIC soil hydrology scheme	Same as VIC	Vegetation data are the same as used in CLM3.5; soil data are the same as in VIC	Wang et al. (2008)

(2005) to determine how different reconstructions of drought properties from different LSMs are over a retrospective period from 1920–2003.

The purpose of this study, therefore, is fourfold: (i) to evaluate the major drought events according to their severity and duration, (ii) to assess the degree of similarity of different LSMs in their reproduction of drought characteristics, (iii) to provide explanations of the physical differences among model products, and (iv) to develop multimodel ensemble techniques for estimation of initial conditions for real-time drought forecasting.

2. Models and data

Six widely used LSMs (note that we broadly interpret the term LSM to include macroscale hydrological models such as VIC) were incorporated into our multimodel ensemble system. They include 1) VIC (Liang et al. 1994);

2) the Community Land Model, version 3.5 (CLM3.5; Oleson et al. 2007); 3) the Noah LSM (Schaake et al. 1996; Chen et al. 1997; Koren et al. 1999; Ek et al. 2003); 4) a catchment-based model (catchment; Koster et al. 2000a; Ducharne et al. 2000), 5) Sacramento/Snow-17 (Sac; Burnash et al. 1973; Anderson 1973), and 6) a hybrid of CLM 3.5 with the VIC soil hydrology scheme (CLM–VIC; Wang et al. 2008). Most of these models have been used as the lower boundary for coupled models or used in previous offline experiments, and their performance has been evaluated in the references noted above. Most have been evaluated in one or more experiments of the Project for Intercomparison of Land-Surface Parameterization Schemes (PILPS). As shown in PILPS experiments such as PILPS-2c (model evaluation over the Arkansas–Red River basin; Wood et al. 1998) the structure and parameterizations of these models differ considerably, as do, in turn, their representations of soil moisture and runoff. Since hydrological drought (runoff) is closely linked to agricultural drought (soil moisture; see Andreadis et al. 2005; Andreadis and Lettenmaier 2006), we focus our attention here on agricultural drought (soil moisture).

Because our goal is to examine the performances of each model's ability to reproduce past drought events in their default condition, the parameters are therefore also model specific. For instance, the soil and vegetation parameters needed for each model were taken from the model's standard setup and provided, where possible, by the model developers. Table 1 summarizes the primary differences among models and the sources of soil and vegetation parameters. All models have a single vegetation layer (except Sac, which does not explicitly simulate vegetation) and at least one snow layer. For different models, the parameterizations of the exchange of energy and water between canopy and the atmosphere above (and below) are also quite different. These parameterizations have been well documented in model technical notes or literature. Therefore, we will not describe the details in this study, but instead refer the reader to the specific studies cited for each model.

All models were run at 0.5° spatial resolution over the land area of the conterminous United States (encompassing a total of 3322 grid cells) for the period 1915–2003. The atmospheric forcing data were the same as in Andreadis et al. (2005) and consisted of daily precipitation, daily wind speed, and daily maximum/minimum air temperature, which were essentially merged from the gridded National Oceanic and Atmospheric Administration (NOAA) Cooperative Observer (Co-op) station data and National Centers for Environmental Prediction (NCEP) reanalysis data. The derivation of the forcing data was described in Andreadis et al. (2005). Because most of the models (except VIC and Sac) only run at subdaily time steps, we disaggregated the daily forcing data to an hourly time step using methods reported in Nijssen et al. (2001).

Maurer et al. (2002) describe an algorithm to stochastically disaggregate daily precipitation into subdaily values, in which the probabilities of time of occurrence and the number of hours of precipitation were derived from the NOAA/National Climatic Data Center (NCDC) Co-op stations that report hourly. They found that the runoff and evapotranspiration simulated by the VIC model were not substantially affected by the diurnal precipitation distribution. To test the sensitivities of the other models to the method of precipitation disaggregation, we subdivided daily precipitation into diurnal quantities using two methods: uniform distribution of daily amounts and the Maurer et al. (2002) approach. With the exception of the catchment model, we found that the monthly simulated soil moisture (which was our main interest in this study) did not exhibit high sensitivity to diurnal precipitation distributions. Specifically, the simulated monthly soil moisture values used in our analysis were very similar regardless of which of the two disaggregation algorithms for daily to subdaily precipitation were used (a similar result was found by Maurer et al. 2002 for VIC). For simplicity, therefore, daily precipitation for all models other than catchment model was disaggregated to hourly by simply dividing the daily precipitation evenly over the entire day; for the catchment model, we used the Maurer et al. (2002) approach. Surface pressure data were adjusted from sea level pressure using a high-resolution digital elevation model and an assumed lapse rate of 0.0065°C m^{-1} with a hydrostatic assumption. To reduce initialization effects, all models were first run for a 10-yr spinup period, consisting of the forcing data from 1915 repeated 10 times, prior to simulation for the period January 1915 to December 2003. All models other than catchment used an hourly time step (catchment used a time step of 20 min). Monthly simulated soil moisture from 1920 to 2003 was then analyzed.

3. Approach

Because different models differ substantially in their representations of hydrological processes, differences in model-predicted soil moisture can be quite large. As an example, Fig. 1 shows the time series of model-simulated total column soil moisture over a grid cell. The tremendous disparities evident in the figure make it clear that direct use of the models' simulated soil moistures, particularly in a multimodel context, is not feasible. Koster et al. (2009, hereafter KGYDM),

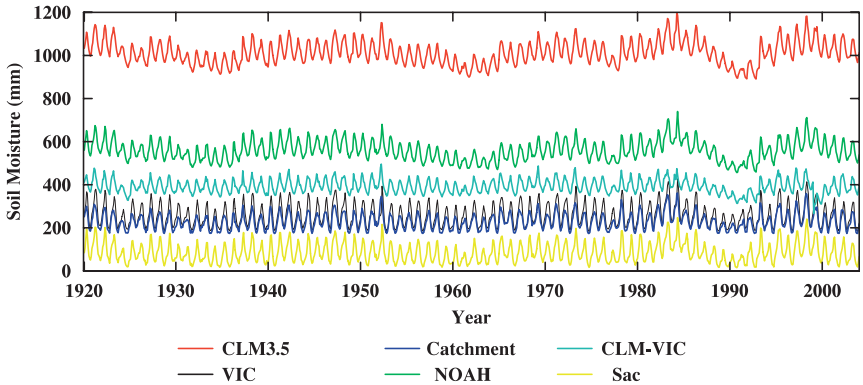

FIG. 1. Monthly time series of simulated total column soil moisture at one grid cell (40.25°N, 112.25°W) from the six models in the study: CLM3.5, VIC, catchment, Noah, CLM–VIC, and Sac.

also motivated by similar intermodel differences in soil moisture, suggested a method to map the simulated soil moisture for multiple models into standard normal deviates, which essentially expresses variations in each model's soil moisture relative to its climatology. An alternative of the KGYDM approach, used by the U.S. Climate Prediction Center (CPC) as well as the University of Washington West-Wide Seasonal Hydrologic Forecast System, is to express soil moisture as percentiles relative to the model's climatology. This results in soil moisture being mapped to a variable that ranges from zero to one and by construct is uniformly distributed for each model. This method is also used by the Climate Prediction Center (2005), which defines drought as occurring when the soil moisture percentile is below 20%. To avoid seasonal biases, we applied the method on a monthly basis; that is, for each grid cell and each month, the percentiles were estimated from the climatology of that month. Using this approach, we transformed the 84 yr (1920–2003) of retrospectively simulated monthly soil moisture into percentiles using the Weibull plotting position algorithm. In the following analysis, we followed the CPC approach of designating soil moisture percentiles below 20% as drought.

Two simple ensemble methods were used to combine soil moisture values from different models: (i) averaging all models' simulated soil moisture percentiles (referred to as ensemble 0) and (ii) normalizing total column soil moisture from the individual models, then averaging over models, and finally calculating the percentiles corresponding to the averaged values (referred to as ensemble 1). In ensemble 1, the normalizing method can be described as $A_{i,\mathrm{nor}} = (A_i - A_{i,\mathrm{min}})/(A_{i,\mathrm{max}} - A_{i,\mathrm{max}})$, where $A_{i,\mathrm{nor}}$ is the normalized value of the monthly soil moisture A_i for grid cell i, and $A_{i,\mathrm{min}}$ and $A_{i,\mathrm{max}}$ are the minimum and maximum values of A_i during the period of 1920–2003, respectively. This results in normalized values ($A_{i,\mathrm{nor}}$) ranging from zero to one. One important difference between these two ensemble methods is that ensemble 1 is expressed as a percentile of its own historical distribution (in similar fashion to the individual models), while ensemble 0 is simply the average of the model percentiles. We expect that, in general, the simple average of ensemble 0 will de-emphasize extremes in comparison to ensemble 1 because of the rarity of all models' percentiles reaching extreme values at the same time. However, in this study, the two ensemble methods tended to yield very similar results. All analyses that follow were performed on all eight time series of percentiles (the six models and the two ensembles).

To investigate the similarities and differences among the models in terms of their representation of droughts, we applied to following analysis to each model: (i) comparisons of the differences of model-simulated soil moisture percentiles; (ii) the SAD relationships; (iii) correlation coefficients among soil moisture (percentiles) simulated by the different models; (iv) the response time of soil moisture (e-folding decay time of soil moisture autocorrelation) simulated by each model; and (v) the correlation coefficients among precipitation, evapotranspiration, soil moisture, and runoff. Aside from the SAD relationships, each of these quantities was computed on a gridcell basis; hence results are presented as maps.

4. Analysis of retrospective multimodel simulations

a. Drought spatial extent and temporal variations

During last century, droughts of the 1930s and 1950s were the most notable for their duration and geographic extent (Schubert et al. 2004b; Cook et al. 1999). As an

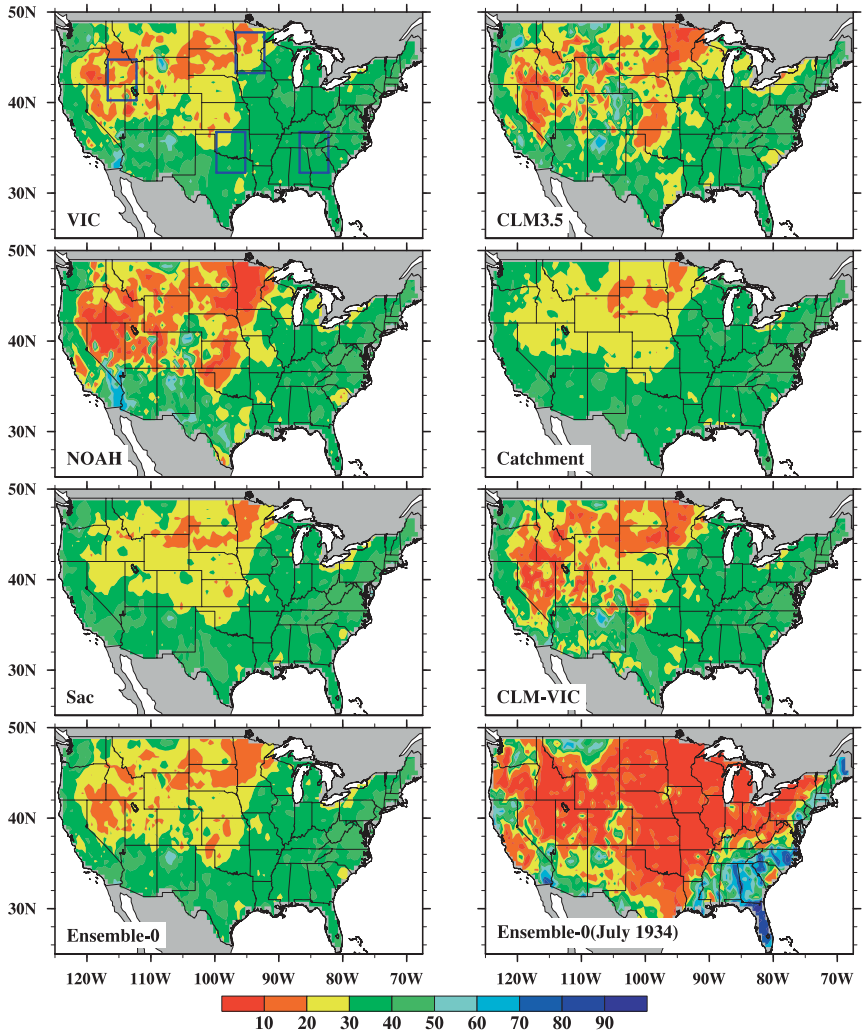

FIG. 2. Spatial distributions of soil moisture percentiles averaged during the period 1932–38 from individual model and ensemble 0, and in July 1934 from ensemble 0. The percentiles were calculated based on the retrospective simulations from 1920 to 2003. The four boxes in the VIC map delineate the four focus regions whose time series are examined in section 4a.

example, Fig. 2 shows the spatial distribution of soil moisture percentiles derived from the six models and ensemble 0 averaged over the period 1932–38 and at the height of the 1930s drought (July 1934) from ensemble 0. All models show an extreme areal extent of drought during this period. At this point, the drought extended across the Great Plains, and also included several western states (Idaho, Wyoming, Nevada, Utah, and eastern Oregon). Among all models, the Noah model has the largest drought spatial coverage, and severe drought (percentiles below 10%) was prevalent over the entire states of Minnesota and Nevada, whereas only parts of these two states experienced drought in the other models. On the other hand, the spatial distribution of drought from the catchment model was the smallest, and was concentrated in the central and western Great Plains, with only scattered patches in the western and eastern states. The map from the ensemble 0 method displays drought extents that were intermediate between those of catchment and Noah. The map for July 1934 from ensemble 0 shows that the drought was prevalent across entire United States except some of coastline regions, and most of drought was extreme severe with the percentile under 10%.

Figure 3 shows the same maps as in Fig. 2 but for the period of 1950–57 and November 1952 from ensemble 0. The drought's areal extent was much smaller compared with the map in Fig. 2 and was concentrated in the New Mexico, southern Texas, and scattered patches in the central and northern states. With respect to severity, the

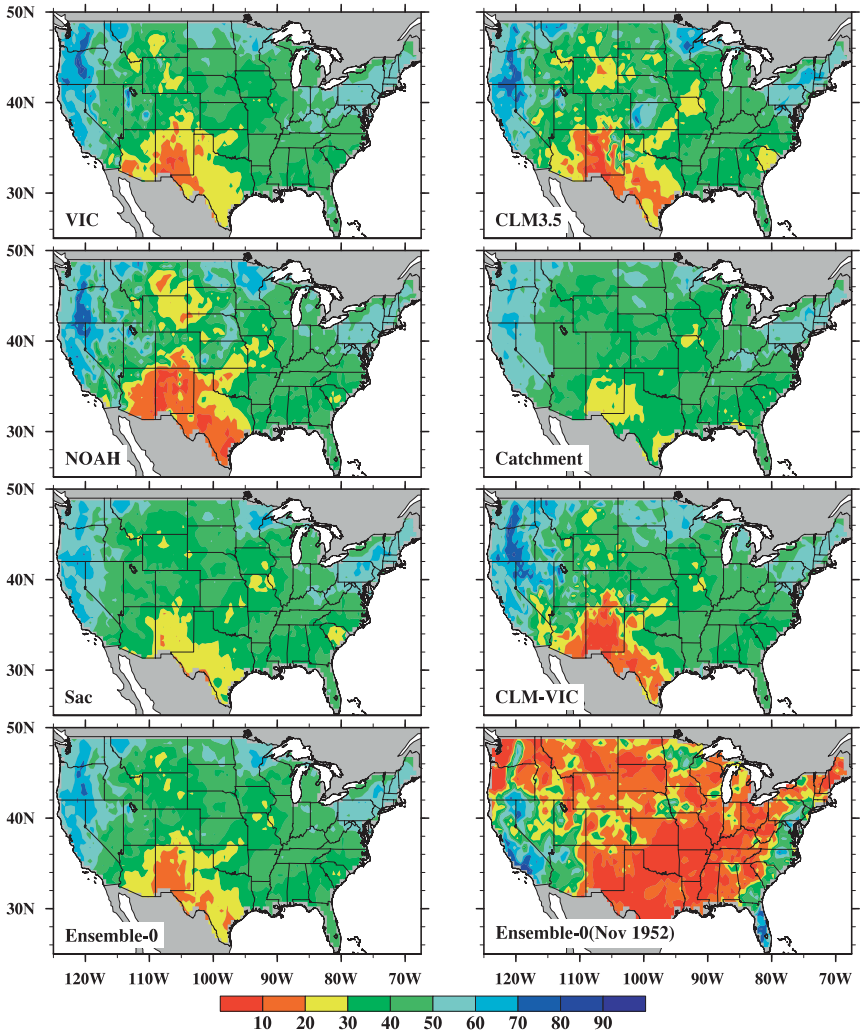

FIG. 3. Same as Fig. 2, but for the period of 1950–57 and November 1952.

severe drought coverage simulated by VIC, CLM3.5, Noah, and CLM–VIC were prominent compared to the rest of the models. Sac and catchment models show the smallest drought spatial coverage and drought severities among all model simulations. The last panel of the Fig. 3 shows that the drought for November 1952 from ensemble 0 spanned across entire United States except some coastline regions. This is consistent with conclusions of others (e.g., Cook et al. 1999).

To demonstrate the temporal evolution of agricultural drought from the different models' simulations, we examined time series of area-averaged soil moisture percentiles from four 5° × 5° regions in the west, north-central, south-central, and southeastern United States (see Fig. 2) as well as the entire conterminous United States. Figure 4 shows the 12-month moving average soil moisture percentiles for the four regions as well as the entire United States for the period 1920–2003 for all models and the two ensemble methods. The 1930s drought is prominent in the west and north-central time series. The 1950s drought is similarly prominent in the south-central and southeast time series. The figure also shows the presence of severe droughts in the west and southeast in the early 2000s.

From the figure, we also can see that both multimodel methods tend to yield results that are intermediate in the range of individual model results (this is guaranteed for ensemble 0 by construct, since it is the average of the individual models). Variations of soil moisture from ensemble 1 are slightly larger than those from ensemble 0, as expected from the fact that ensemble 0 is not reexpressed as a percentile of its own historical distribution. For the most part, differences between the two ensemble methods are small. Notable exceptions

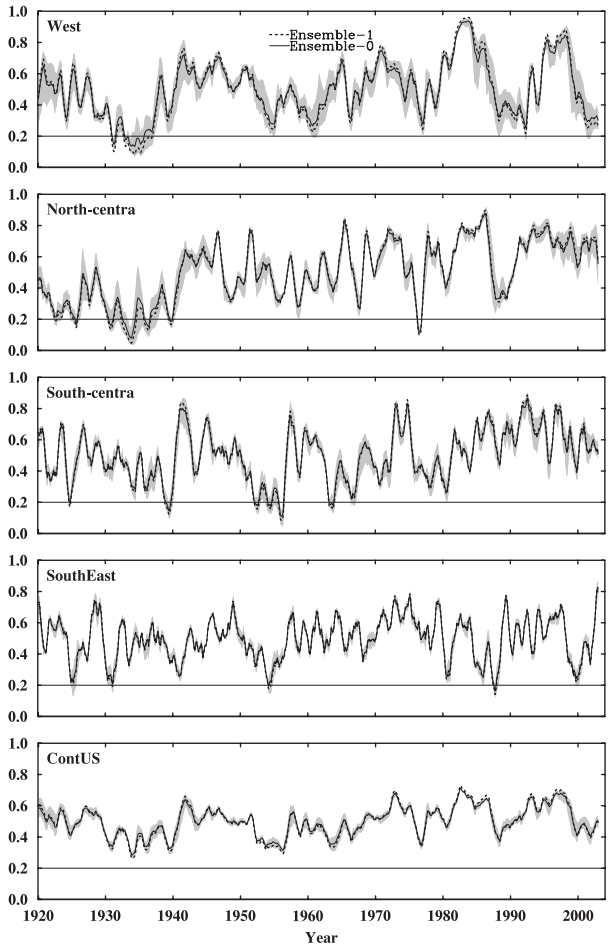

FIG. 4. Monthly soil moisture percentiles averaged over the areas of four boxes shown in Fig. 2 (VIC) and over the whole contiguous United States. The curves shown in the figure are 12-month moving averages. For each box, we have plotted the envelope of the percentiles from all models (shown in gray shadow) and the percentiles from the two ensemble methods (shown in solid and dash lines). The lines of 20th percentile are also plotted on each panel.

include differences of approximately 5% for the 1930s drought in the west and north-central regions, and other extreme dry and wet periods in the west during the 1950s, 1980s, 1990s, and early 2000s. During these periods, ensemble 1 falls near an extreme end of the range.

Figure 5 shows the soil moisture percentiles for 1930s. The most severe portion of the 1930s drought occurred in mid-1934, with average percentiles below 10% in all four regions, making it clear why this event is often referred to as the ''drought of the century'' (Schubert et al. 2004b). Among the six models' simulated soil moisture percentiles, simulations from the CLM3.5 model have the least variation, and the catchment model has largest variation across most of the regions. This may be because of the relatively high water-holding capacity of CLM3.5 relative to the catchment model (Fig. 6); a shallow water-holding capacity is more easily affected by atmospheric conditions (this will be addressed in more detail in section 4d). Results for the 1950s drought (figure not shown) were similar with respect to among-model variations.

b. *Severity–area–duration analysis*

SAD analysis, as described in Andreadis et al. (2005), provides a means of showing relationships among the maximum area covered by drought for a given duration and (space–time) average severity (here the average of the total column soil moisture percentile). Based on a simple clustering algorithm that incorporates spatial contiguity, the SAD analysis first groups the monthly soil moisture time series into a number of clusters and then merges those clusters under minimum area constraints. Andreadis et al. (2005) describe the search algorithms and protocols used to define contiguous drought areas. Using the SAD approach, the most severe events for each duration and area covered from 1920 to 2003 were identified. The SAD curves are essentially envelopes, and it is possible as a subsequent step to determine which drought events contribute to the various points on the envelope curves. Figure 7 shows the SAD envelope curves for the different LSMs and the two ensemble methods. For all models, the 1930s drought covers a substantial portion of the SAD space, even though the durations at which these maximal severities occurred differed among the models. In contrast to the other models, CLM3.5's simulation of the 1930s drought was the most dominant event in all durations, with the early 2000s drought appearing only for relatively small areas. It also can be seen that the 1930s drought in CLM3.5 lasted the longest. This may well be explained by the deep total soil column in CLM3.5, which results in longer soil moisture persistence as compared with the other models (the issue of soil moisture persistence is addressed further in section 4d). In general (except for ensemble 0), all models showed that the drought of the late 1990s to early 2000s was the most severe for small areas (smaller than 2×10^6 km^2). In most of the models, the 1950s drought was second in prominence to the drought of the 1930s, and most models (except for CLM3.5 and Noah) showed this drought appearing at the longer durations (12 months or longer) and areas expanded up to 7×10^{-6} km^2. The literature also indicates the occurrence of a drought in the mid-1970s (e.g., Wilhite 1983), but from our simulations only three models (Noah, Sac, and catchment models) showed that this drought event contributed to the SAD envelope curves for small areas.

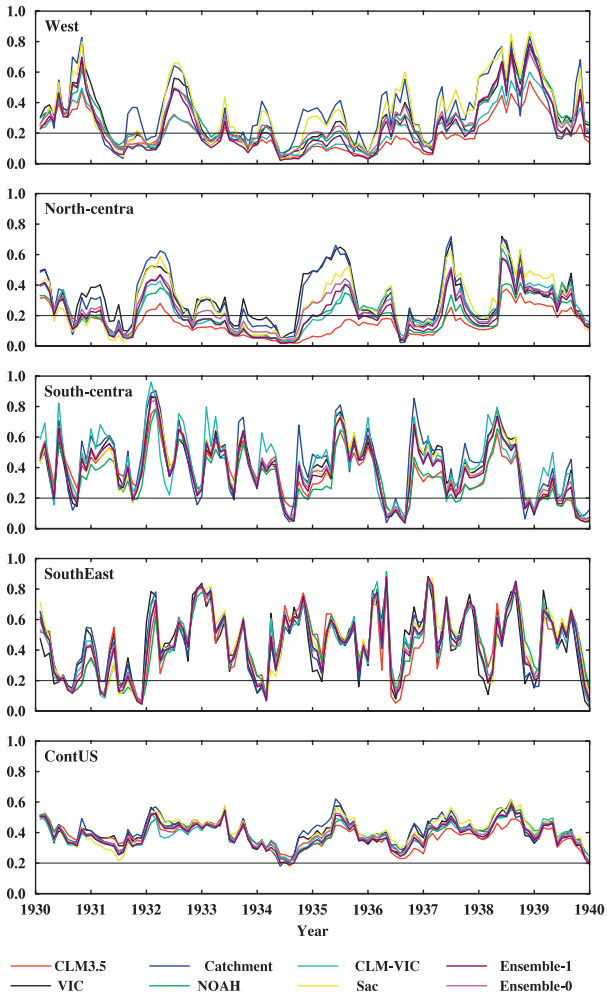

FIG. 5. Monthly soil moisture percentiles averaged over the areas of four boxes shown in Fig. 2 (VIC) and over the whole contiguous United States. For each box, we have plotted the percentiles from all models (shown in gray shadow) and the percentiles from the two ensemble methods (shown in solid and dash lines). The lines of 20th percentile are also plotted on each panel.

It should be noted that SAD technique considers the area of the drought, which differs from model to model, and thus the SAD curves differ, even though the selected time series from points in the centers of the droughts may appear similar among the models (Fig. 4). Differences among the individual models are especially apparent when considering the range of drought severity for a given area (or the range of area for a given severity). In Fig. 7, CLM3.5's SAD curves occupy the narrowest range of severity for a given area, while those from the catchment model occupy the widest range. As we might expect, the two multimodel ensemble plots show an intermediate range of severity for a given area. If we interpret the range of severity for a given area as an indication of the sensitivity of simulated drought to climatic conditions and antecedent soil moisture, then the multimodel ensembles tend to have an intermediate sensitivity compared to the individual models. Whether this is a more accurate representation of the areal extents of these droughts is not clear, given the absence of an observational basis for comparison.

c. *Correlation coefficients between models' simulated soil moisture*

KGYDM used the cross-correlation coefficients (ρ) among pairs of models as a means of characterizing similarities in their dynamic variability. We used the same approach, where ρ for each model pair was based on the time series of monthly soil moisture percentiles for the two models. Larger ρ values indicate more agreement between the pair of models. Table 2 shows ρ values, computed from the entire 84-yr period and averaged over all grid cells, for each of the 15 pairs of models (the values in parentheses are for the two periods of 1932–38 and 1950–57, respectively). All ρ values were larger than 0.6; the smallest value (0.67) was from the CLM3.5 and catchment pair, and the largest value was from the Noah and Sac pair. During the two extreme drought periods (i.e., 1930s and 1950s), the ρ values are also comparable to values calculated from the whole 84-yr period. The values in Table 2 suggest that the models generally agreed with each other in terms of the simulated soil moisture, although the similarities of some pairs of models are more pronounced than others. We also examined the spatial distribution of model agreement. For each grid cell, we averaged the ρ values of all 15 model pairs. Figure 8a) shows the spatial distribution of the averaged ρ for the periods of 1920–2003. The Great Plains clearly divides the ρ map into two parts, with the ρ values in the western part smaller than in the eastern part. The ρ values in most of the west are smaller than 0.8 except for some larger values appearing along the northwest coast, while in most of the east the ρ values are larger than 0.8, and in particular are larger than 0.9 over parts of Indiana, Missouri, and Illinois. Over the Great Plains, the ρ values mostly are the range 0.7~0.8. Figure 8b, which shows spatial variations in the standard derivation of annual precipitation during the period 1920–2003, shows that precipitation variations over the eastern United States tend to be larger than over the western United States (note that, because annual average precipitation is larger over the eastern United States than the western United States, the coefficient of variation of annual precipitation actually decreases from west to east). There is a close correspondence between ρ and the variance of annual precipitation (e.g., Fig. 4 of Koster et al. 2000b). In areas for which the precipitation varies greatly from

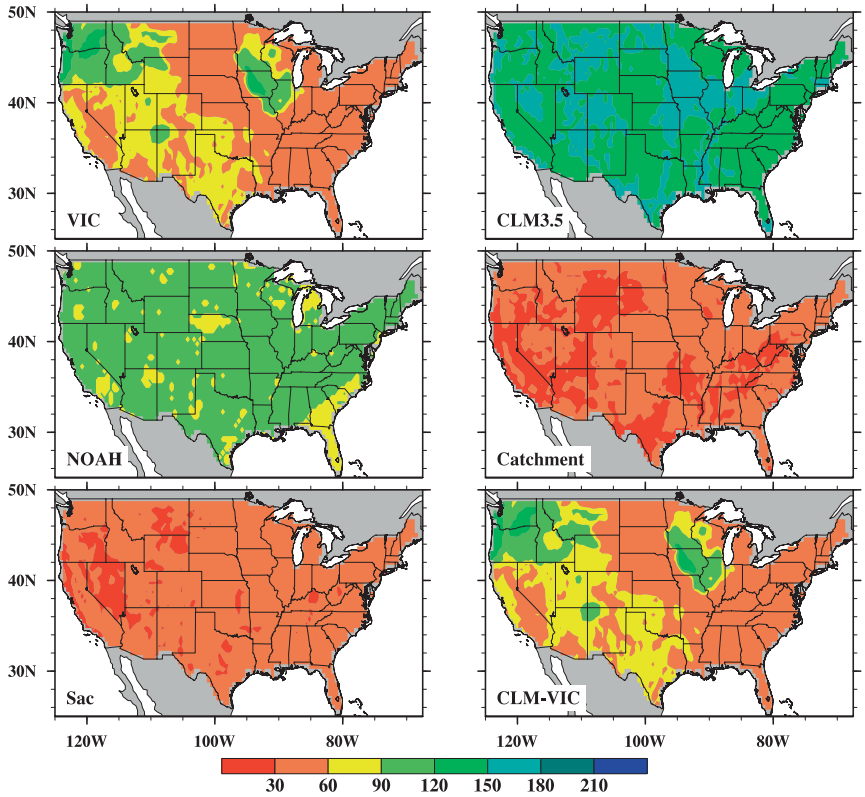

FIG. 6. Map of soil water–holding capacity from the models used in this study. Note that the water-holding capacity of the catchment model includes only water in excess of the wilting point.

year to year, the interannual variations of soil moisture should also be large, and large variations are easier for all models to capture than are small variations. The averaged ρ map for the periods 1932–38 and 1952–57 are similar as Fig. 8 (figures not shown).

d. *Response time of soil moisture*

To investigate the persistence of soil moisture, we calculated the response times implicit in the soil moisture time series. Response time is defined here as the lag time at which the autocorrelation of the time series of soil moisture has decayed to 1 e^{-1} (Delworth and Manabe 1988). Figure 8 shows the spatial distribution of soil moisture response times computed from the percentile time series for the period 1920–2003. The models show a wide disparity in response times, particularly in the western United States, with the catchment and Sac models showing low values (less than 1 yr) and the other models showing response times as high as several years.

Previous work has shown that soil moisture memory is related to soil depth and soil characteristics (e.g., porosity and texture), with deeper soil moisture producing longer memory than shallower layers (Wang et al. 2006). Indeed, the differences seen in Fig. 9 relate directly to differences in the models' total water-holding capacities—how deep into the soil the precipitation signal is allowed to penetrate. The figure clearly shows that the models with the largest soil water-holding capacities (i.e., Fig. 6) also have the largest response times (i.e., Fig. 9). In addition, Fig. 9 shows that soil moisture simulated from most models except catchment and Sac is more persistent in the interior of the United States than on the East and West Coasts, which, to some extent, is consistent with one of Karl's (1983) early findings—"spells of abnormally wet or dry weather have more persistence in the Rocky Mountain and High Plains states than states farther east or west."

The above analyses are based on temporal or spatial averages, which tend to reduce the variations of the variables. To explore the relationship between precipitation and soil moisture in finer spatial detail, we chose two points (indicated on Fig. 9) from the simulations of CLM3.5 and Sac that represent two extreme cases of arid and wet conditions. The top two panels of Fig. 10 illustrate this with a comparison of Sac and CLM3.5 relative soil moisture (i.e., ratio of total column soil

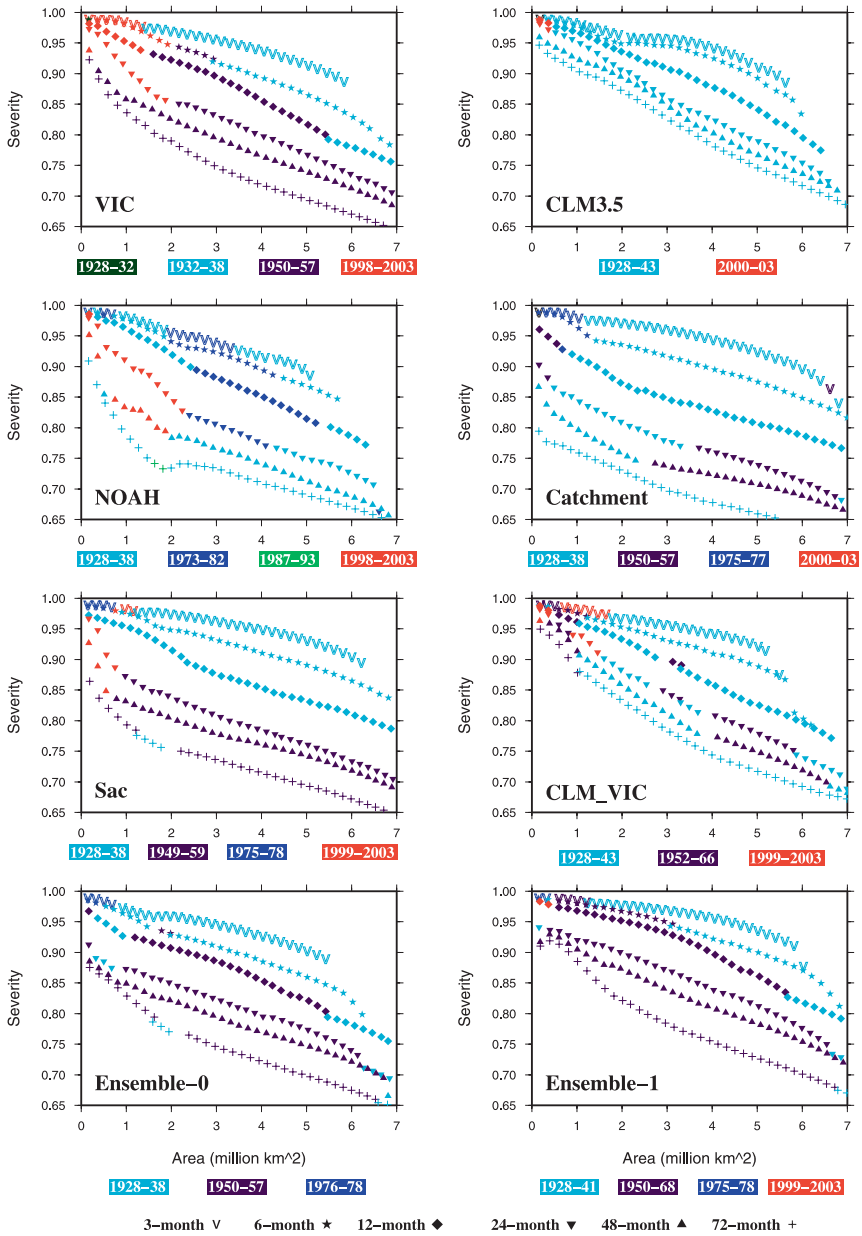

FIG. 7. The maximum severities of drought events at the different durations (3, 6, 12, 24, 48, and 72 months) derived from soil moisture simulated by the different models and the two ensembles. Different markers correspond to different durations, and different colors correspond to different specific drought events.

moisture to soil-holding capacity) for an extreme case, a western point for which the time series of annual rainfall shows, on average, a long-term dip between 1930 and 1985. The CLM3.5 clearly transforms this multidecadal-scale variability in the precipitation forcing into a corresponding multidecadal-scale variability in total soil moisture. Furthermore, the dip in soil moisture for CLM3.5 during the middle of the century is more pronounced than that of precipitation because the soil moisture variable filters out higher frequencies of rainfall variability (Delworth and Manabe 1988). For CLM3.5, it is this multidecadal-scale dip—this manifestation of long-term variability in the model forcing—that is primarily responsible for the high response time (*e*-folding time) seen in Fig. 9 at this point.

Now consider the Sac model, for which the total water-holding capacity is much smaller (about 30 cm at this point as opposed to almost 144 cm for CLM). The

TABLE 2. Correlation coefficients among models' simulated soil moisture percentiles. Values in parentheses are for the periods 1932–38 and 1950–57, respectively.

Model	VIC	CLM3.5	Noah	Sac	Catchment	CLM–VIC
VIC	1					
CLM3.5	0.71 (0.69, 0.71)	1				
Noah	0.75 (0.74, 0.76)	0.83 (0.82, 0.83)	1			
Sac	0.81 (0.78, 0.79)	0.76 (0.75, 0.75)	0.84 (0.85, 0.84)	1		
Catchment	0.79 (0.77, 0.78)	0.67 (0.65, 0.67)	0.74 (0.75, 0.76)	0.87 (0.86, 0.87)	1	
CLM–VIC	0.75 (0.73, 0.75)	0.79 (0.81, 0.83)	0.76 (0.78, 0.78)	0.76 (0.77, 0.75)	0.71 (0.70, 0.71)	1

smaller water-holding capacity means that the midcentury dip in rainfall cannot affect the soil moisture as much; the soil moisture is already close to zero prior to the dip in rainfall, and it cannot get much drier than that once the lower rainfalls begin. The soil moisture recovers quickly once the larger rains return, and overall, the year-to-year soil moisture variations appear to be of the same order as the multidecadal-scale variations. These properties point to a much smaller response time.

Why, then, does a model like CLM, with its large water-holding capacity, show low response times in the eastern United States? An answer is suggested by the bottom two panels in Fig. 10, which show the same type of comparison for an eastern point (soil-holding capacity: about 49 cm for the Sac model and 148 cm for CLM). Here, conditions are generally wet enough that, even in relatively dry years, the soil moisture remains near the high end, as defined by saturation (or possibly field capacity). (Though total soil moisture does decrease seasonally with summer evaporation, it apparently recovers easily with winter precipitation.) For either model, the large, decadal-scale positive rainfall anomaly in the 1940s cannot manifest itself in the total soil moisture because the soil is already about as wet as it can be—again, even for relatively dry years. As a result, the soil moisture response time at this eastern point does not reflect the long-term variability of the forcing.

e. Relationship between hydrological variables

To investigate the possible reasons for the differences among the models' simulated soil moisture, we calculated the area-averaged correlation coefficients between the precipitation forcing and the models' simulated hydrological variables (soil moisture, evapotranspiration, and runoff), and examined the water balance for the period 1920–2003. For each month, the water balance equation at the land surface can be expressed as $\Delta SM = P - E - R - \Delta SWE$, where ΔSM is the net change in soil water storage over the month and P, E, R, and ΔSWE are the total precipitation, evapotranspiration, runoff, and the changes of snow water equivalent if snow is present for that month, respectively. In this work, P is the same for all models, and therefore the changes in water storage are determined primarily by E, R, and ΔSWE. From the long-term point of view, ΔSWE would be turned into E, R, or SM and ΔSM does not change much, therefore ΔSWE and ΔSM can be considered negligible. The spatially averaged correlation coefficients among P, SM, E, and R are shown in Table 3. In general, runoff was much more highly correlated with P than with the other variables except for CLM3.5, probably because of its large water-holding capacity in the deeper soil layers, which are less affected by atmospheric conditions, as mentioned above. The positive sign of the correlation coefficients usually reflects a feedback relationship between the two quantities. For example, catchment and VIC showed the highest correlation between P and R among the models, implying that R was more efficiently responsive to P than for the other models. The relationship between soil moisture and E largely depends on transpiration removing soil water from the root zone layer and bare soil evaporation. The root distribution within soil is one of the factors that determine transpiration. The catchment and Sac models show higher correlation coefficients between E and soil moisture than do the other models. In the case of catchment, the reason may be that the soil water removal by transpiration is more prominent than in other models. But the Sac model does not explicitly include a vegetation layer. The Sac model's evaporation is a bulk computation that results in moisture being extracted directly from subsurface storage. From Fig. 2 of Mitchell et al. (2004), Sac shows larger evaporation than VIC and Noah in the North American Data Assimilation Systems (NLDAS) simulations. Given that we employ the NLDAS soil parameters for the Sac and Noah models in this study as well, the high correlation observed between the Sac model's E and soil moisture may be due to the choice of soil parameters, expressed through Sac's soil evaporation.

Also shown in Table 3 are the runoff coefficients computed as the ratio of simulated total runoff to total precipitation over the United States for each model. For reference purposes, for the period 1950–2000, the

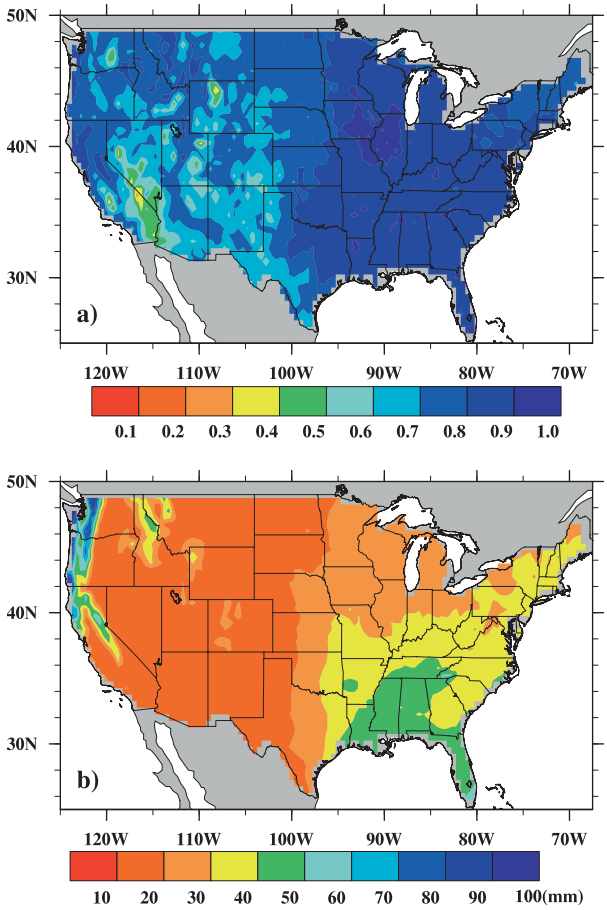

FIG. 8. (a) Averaged correlation coefficients between soil moisture percentiles from all pairs of model simulation over the period of 1920–2003 and (b) the std variation of annual precipitation for the period of 1920–2003.

inferred runoff ratio is about 0.26, based on VIC simulations in which model runoff was calibrated to observations (Maurer et al. 2002). Especially for Noah and catchment (and to a lesser extent, Sac), the relatively low simulated runoff ratios may also suggest that runoff production is somewhat less dynamic than in the other models. On the other hand, comparison of the simulated runoff ratios with precipitation–runoff correlations does not support such a hypothesis in general.

5. Application to real-time hydrological nowcast

The techniques outlined have been implemented into a real-time drought nowcast system over the continental United States, as an extension to the University of Washington's Surface Water Monitor (Wood 2008). This system originally was based around the VIC model alone, we report here an expansion that includes three additional models: Noah, Sacramento/Snow-17, and CLM3.5.

The system produces daily "nowcasts" of soil moisture, consisting of a simulation spanning a time window from an initial model state 1–2 months prior to the current day, up through the day before the current day (the prior 1–2 months are rerun each day to allow incorporation within the model forcing data of gridded station data that incorporate stations not available in real time but that become available later). Meteorological forcings during this window are computed via the index station method described in Tang et al. (2009). All models use the same set of meteorological forcings as input. Sac requires potential evapotranspiration (PET) as an additional input, which is taken from the corresponding Noah simulation as in Mitchell et al. (2004). Soil and vegetation parameters for all models are the same as in the retrospective simulations. Simulated total column soil moisture from each model is converted into percentiles relative to that model's retrospective monthly climatology. Although there is a minor issue in comparing current daily soil moisture to the historical distribution of monthly average values for the current month, and alternative approaches could be used, the inherent error is small, and we prefer not to effectively average conditions over a window leading up to the current day (which would remove the problem) in the interest of obtaining an estimate of the current days' conditions. We use an ensemble average that is similar to ensemble 1 described above, with the exception that the individual models' percentiles (rather than normalized soil moistures) are used to construct the average, which is then converted into a percentile of its historical distribution.

Figure 11 shows soil moisture percentiles for the four individual models, and the multimodel averages for 1 November 2007, 1 December 2007, and 1 January 2008. Evolution of a well-publicized drought over the southeastern United States, centered on Georgia, is of particular interest. Over this region, VIC shows a notably less extensive, and less persistent, drought than the other models, and Noah is more extensive and persistent than the other models. CLM3.5 and Sac are intermediate. It is interesting that VIC and Sac, and to a lesser extent CLM3.5, show the drought essentially gone over Georgia by 1 January, whereas Noah shows it persisting. The multimodel mean also shows the drought gone by 1 January. Similarly, while all models agree in general that dry conditions exist in California and Nevada during at least part of this period, the fluidity with which these conditions change varies across the set of models. The model having the most persistent soil moisture in this case is CLM 3.5, whose dry areas appear virtually static for the entire period. At the other extreme, Sac's dry areas along the West Coast bear little

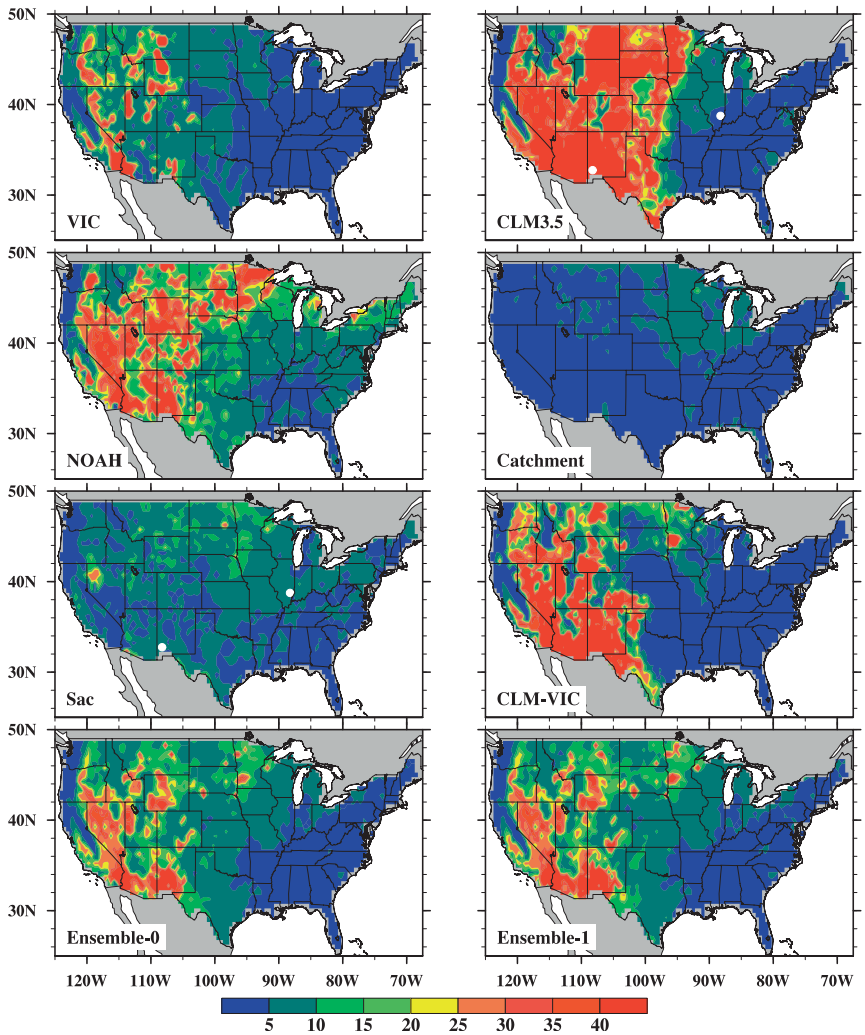

FIG. 9. Spatial distribution of the response time (months; *e*-folding decay time of autocorrelation) of model-simulated soil moisture.

resemblance to each other from one month to the next. On the other hand, the individual models agree more strongly with respect to wetter than normal conditions in the Great Plains. It is easier to see the evolution of conditions in these regions on the multimodel map because of the removal of "noise" from the individual models. In the context of real-time monitoring, such behavior can be beneficial, as it reduces the sensitivity of the ensemble to uncertainty in the real-time meteorological forcings.

As noted above in our discussion of the retrospective simulations, the soil moisture response times vary considerably, not only among models, but also geographically (Fig. 9). In the case of the drought in the Southeast, model response times are more or less similar, while in the Great Plains and on the West Coast model response times exhibit a wider range. The stronger agreement among models with respect to wet conditions in the Great Plains may stem from the fact that precipitation events can recharge a soil column within a matter of days, bringing all models up to more or less saturated conditions, regardless of differences among model parameterizations, while dry periods, which require drainage and evapotranspiration to empty the soil column, bring out the differences among models (even in the case of the Southeast drought, where soil-holding capacities are similar, but other parameters, such as evapotranspiration, may differ). Thus, we may expect greater uncertainty from the multimodel ensemble under dry conditions (or dry regions such as the western United States, where year-to-year water storage is an important issue) than under wet conditions.

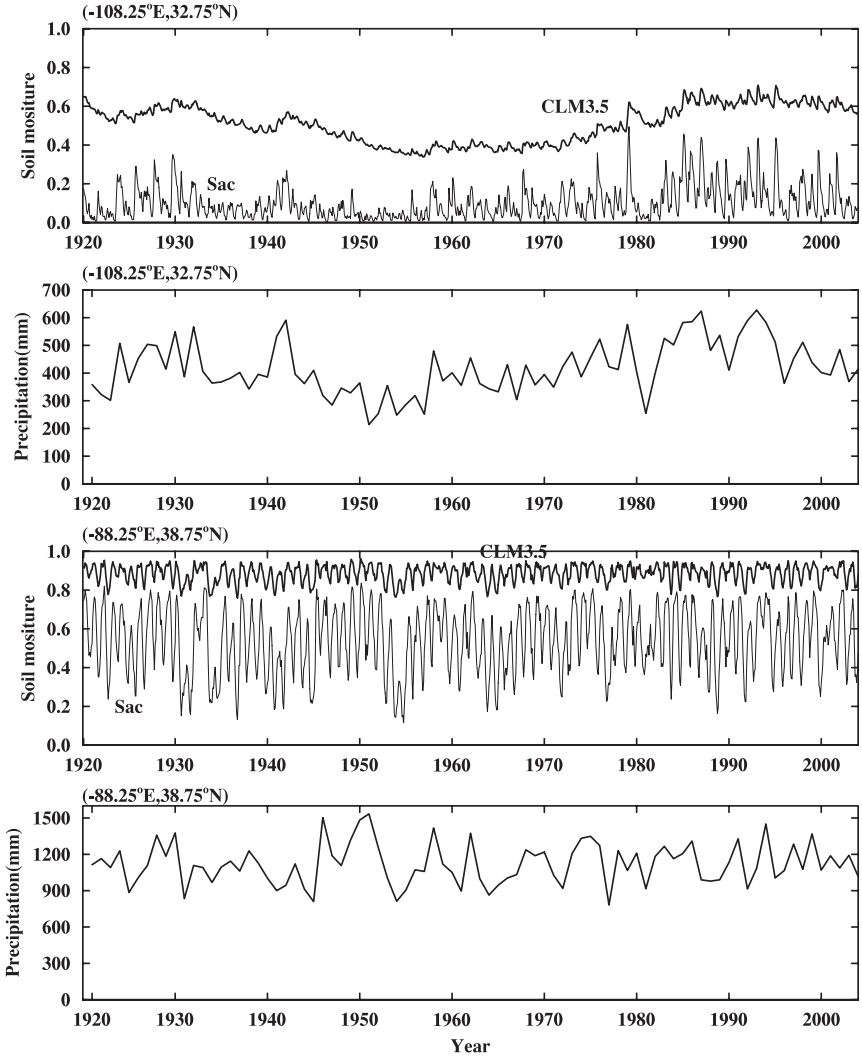

FIG. 10. (a) Time series of monthly relative soil wetness for CLM3.5 (bold curves) and Sac (light curves) for a point in the southwestern United States. The relative soil wetness was from the ratio of total column soil moisture to soil water-holding capacity at the specific point. (b) Time series of annual precipitation at this point. (c), (d) Same (a), but for a point in the eastern United States.

TABLE 3. Spatially averaged correlation coefficients between precipitation (prec) and model-simulated variables [evapotranspiration (evap), runoff, and soil moisture (soilm)] and runoff ratios computed from model-simulated runoff.

Model	Prec and evap	Prec and soilm	Prec and runoff	Evap and soilm	Runoff and soilm	Runoff ratio
VIC	0.44	0.38	0.62	0.46	0.64	0.25
CLM3.5	0.36	0.26	0.31	0.22	0.41	0.17
Noah	0.49	0.28	0.42	0.53	0.45	0.088
Sac	0.39	0.38	0.51	0.54	0.62	0.16
Catchment	0.39	0.38	0.58	0.58	0.48	0.10
CLM–VIC	0.51	0.32	0.51	0.26	0.65	0.31
Average	0.43	0.33	0.49	0.43	0.54	0.18

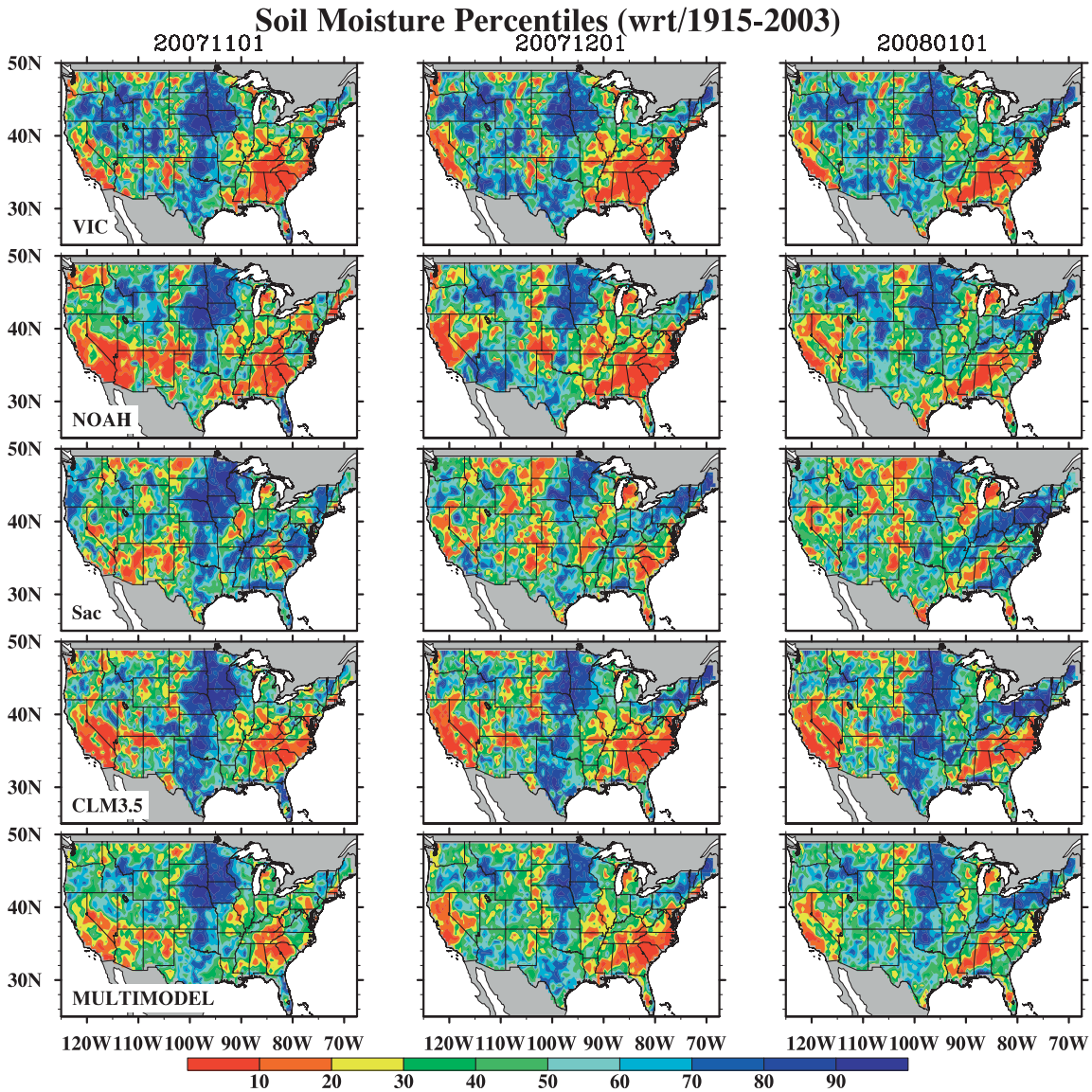

FIG. 11. Soil moisture percentiles for the models VIC, Noah, SAC, CLM3.5 (CLM), and the multimodel average, for the dates 1 Nov 2007, 1 Dec 2007, and 1 Jan 2008.

6. Discussion

As described in section 2, large disparities exist in the parameterization processes incorporated in the various LSMs, and the differences shown in the previous sections are complicated and not easy to explain. Model intercomparison projects such as PILPS have investigated many products of model simulations in various ways, and the results still showed large disparities among different models. Even so, all models' results are plausible in their reproduction of the major agricultural drought events over the conterminous United States during the period 1920–2003.

The differences among model behaviors can be attributed to a number of causes. For the identification of drought as studied here, differences in soil water-holding capacities among the models are clearly one of the major reasons. On the other hand, model parameters (e.g., those model parameters related to soil and vegetation) are a major cause of intermodel differences, and in fact the same model with different parameters may produce quite different results. Exploration of the parameter spaces for each model was not feasible, so instead we made the pragmatic decision to use fixed parameters for the different models, taken where possible from the North American Land Data Assimilation

(NLDAS; Mitchell et al. 2004). Even though most vegetation parameters are derived from satellite data, and soil parameters are derived from high-resolution soil texture data, some uncertainties are inevitable. Another limitation of this study is that we did not consider land use change during the last century. Some studies have shown that land cover change can lead to surface cooling and reduce the diurnal ranges of surface temperature (e.g., Bonan 1997; Matheussen et al. 2000; Oleson et al. 2004)—although it should be noted that the historic forcing data (although not vegetation characteristics) would have reflected such changes.

In all of our analyses, the multimodel ensembles tended to yield results that were intermediate within the range of the individual models. This was more true for ensemble 0 (by construct) than for ensemble 1. Since ensemble 1 was expressed as a percentile of its own historical distribution in the same manner as the individual models, it is arguably a more appropriate method to use when comparing with the individual models. However, this method is more sensitive to the coherency of the individual models than ensemble 0. For example, during events for which the majority of the models yield low percentiles (e.g., the 1930s drought in Fig. 4), ensemble 1 will yield a percentile lower than the average of the individual model percentiles, because of the rarity of agreement among all the models within their historical distribution. Without more comprehensive soil moisture observations, the questions of whether the range of model results is a good measure of model uncertainty and whether ensemble 1's sensitivity to model agreement is a more skillful predictor of actual soil moisture conditions than the method of ensemble 0 are still open. Nevertheless, in this study, differences between the two ensemble methods tended to be small.

7. Summary and conclusions

We used six LSMs to retrospectively simulate soil moisture for the period 1915–2003 over the conterminous United States. All model simulations were performed at 0.5° resolution. The atmospheric forcing data were interpolated from station data, and vegetation and soil parameters were from the standard packages of each model. Simulated monthly soil moisture was converted to percentiles via empirical probability distribution functions for each model. The percentiles were used to represent drought events. Differences among model-simulated soil moisture were evaluated by comparisons of between-model correlation coefficients, the response time of soil moisture, and severity–area–duration analysis. Two ensemble methods were developed to combine the six models' simulations. To further evaluate the relationships among hydrological components from model simulations and precipitation, we calculated the correlation coefficients between precipitation, soil moisture, evapotranspiration, and runoff.

Our major conclusions are the following:

1) All six models and the two ensembles all identified the spatial patterns of major drought events during the period 1920–2003 over the conterminous United States. The spatial patterns of severities and duration for severe drought events from all models were plausible, albeit disparities exist between different models' simulations. For example, the 1930s drought event has the longest duration and most severities in CLM3.5 compared to other drought events.
2) The models' simulations were more in agreement with each other over the eastern than over the western United States, probably because the models can agree more easily when forced with larger interannual rainfall amounts. Note here that Sac and catchment have the lowest water-holding capacities.
3) The persistence of soil moisture from different models showed longer retention times of soil moisture over the western than the eastern United States. The model with the deepest soil column (i.e., CLM3.5) generally had the longest soil moisture memory, while the Sac and catchment models had the shortest soil moisture memory.
4) As a preliminary test, the techniques of multimodel ensemble to retrospectively reconstruct the drought have been implemented into a real-time drought nowcast system over the continental United States, as an extension to the University of Washington's Surface Water Monitor.
5) Given the lack of the long-term soil moisture data, we speculate that the products of the multimodel simulations provide a better way to study the long-term hydrological variations of the land surface, especially in studies of drought, than using a single model. Using multiple models in a nowcast system could contribute to the monitoring of the current state of soil water. A useful application of the methodology employed in this work could be applied to evaluate the susceptibility of the United States to drought, and for estimation of drought recovery probabilities in the future.

Acknowledgments. The work was supported by the U.S. Department of Energy under DOE Agreement Number DE-FG02-04ER63873 to the University of Washington, and the CAS Fund (KZCX2-YW-217) at the Institute of Atmospheric Physics. We appreciate the assistance of Ben Livneh of the University of

Washington Land Surface Hydrology Group, who performed the Sac and Noah model simulations.

REFERENCES

Alley, W. M., 1984: The Palmer Drought Severity Index: Limitations and assumptions. *J. Climate Appl. Meteor.,* **23,** 1100–1109.

AMS Council, 1997: Policy statement—Meteorological drought. *Bull. Amer. Meteor. Soc.,* **78,** 847–849.

Anderson, E. A., 1973: National Weather Service River Forecast System: Snow accumulation and ablation model. NOAA Tech. Memo. NWS Hydro-17, 217 pp.

Andreadis, K. M., and D. P. Lettenmaier, 2006: Trends in 20th century drought over the continental United States. *Geophys. Res. Lett.,* **33,** L10403, doi:10.1029/2006GL025711.

——, E. A. Clark, A. W. Wood, A. F. Hamlet, and D. P. Lettenmaier, 2005: Twentieth-century drought in the conterminous United States. *J. Hydrometeor.,* **6,** 985–1001.

Bonan, G. B., 1997: Effects of land use on the climate of the United States. *Climatic Change,* **37,** 449–486.

——, S. Levis, L. Kergoat, and K. W. Oleson, 2002: Landscapes as patches of plant functional types: An integrating concept for climate and ecosystem models. *Global Biogeochem. Cycles,* **16,** 1021, doi:10.1029/2000GB001360.

Burnash, R. J. C., R. L. Ferral, and R. A. McGuire, 1973: A generalized streamflow simulation system: Conceptual modeling for digital computers. National Weather Service and California Department of Water Resources Joint Tech. Rep., 204 pp.

Chen, F., Z. Janjic, and K. Mitchell, 1997: Impact of atmospheric surface layer parameterizations in the new land-surface scheme of the NCEP mesoscale Eta model. *Bound.-Layer Meteor.,* **85,** 391–421.

Climate Prediction Center, cited 2005: U.S. soil moisture monitoring. National Weather Service. [Available online at http://www.cpc.ncep.noaa.gov/soilmst/.]

Cook, E. R., D. M. Meko, D. W. Stahle, and M. K. Cleaveland, 1999: Drought reconstructions for the continental United States. *J. Climate,* **12,** 1145–1162.

Dai, A., K. E. Trenberth, and T. Qian, 2004: A global data set of Palmer Drought Severity Index for 1870–2002: Relationship with soil moisture and effects of surface warming. *J. Hydrometeor.,* **5,** 1117–1130.

Delworth, T. L., and S. Manabe, 1988: The influence of potential evaporation on the variabilities of simulated soil wetness and climate. *J. Climate,* **1,** 523–547.

Ducharne, A., R. D. Koster, M. J. Suarez, M. Stieglitz, and P. Kumar, 2000: A catchment-based approach to modeling land surface processes in a general circulation model. *J. Geophys. Res.,* **105,** 24 823–24 838.

Ek, M. B., K. E. Mitchell, Y. Lin, E. Rogers, P. Grunmann, V. Koren, G. Gayno, and J. D. Tarpley, 2003: Implementation of Noah land surface model advances in the National Centers for Environmental Prediction operational mesoscale Eta model. *J. Geophys. Res.,* **108,** 8851, doi:10.1029/2002JD003296.

Karl, T. R., 1983: Some spatial characteristics of drought duration in the United States. *J. Climate Appl. Meteor.,* **22,** 1356–1366.

——, 1986: The sensitivity of the Palmer Drought Severity Index and Palmer's Z-index to their calibration coefficients including potential evapotranspiration. *J. Climate Appl. Meteor.,* **25,** 78–86.

Keyantash, J., and J. A. Dracup, 2002: The quantification of drought: An evaluation of drought indices. *Bull. Amer. Meteor. Soc.,* **83,** 1167–1180.

Koren, V., J. Schaake, K. Mitchell, Q. Duan, F. Chen, and J. Baker, 1999: A parameterization of snowpack and frozen ground intended for NCEP weather and climate models. *J. Geophys. Res.,* **104,** 19 569–19 585.

Koster, R. D., M. J. Suarez, A. Ducharne, M. Stieglitz, and P. Kumar, 2000a: A catchment-based approach to modeling land surface processes in a general circulation model 1. Model structure. *J. Geophys. Res.,* **105,** 24 809–24 822.

——, ——, and M. Heiser, 2000b: Variance and predictability of precipitation at seasonal-to-interannual timescales. *J. Hydrometeor.,* **1,** 26–46.

——, Z. Guo, R. Yang, P. Dirmeyer, and K. Mitchell, 2009: On the nature of soil moisture in land surface models. *J. Climate,* in press.

Liang, X., D. P. Lettenmaier, E. F. Wood, and S. J. Burges, 1994: A simple hydrologically based model of land surface water and energy fluxes for general circulation models. *J. Geophys. Res.,* **99,** 14 415–14 428.

Martz, J., B. Richardson, and J. M. Souby, 2003: Letter to bill supporters commending introduction of National Drought Preparedness Act of 2003. Western Governors' Association, 2 pp. [Available online at http://www.westgov.org/wga/testim/drought-legis7-24-03.pdf.]

Matheussen, B., R. L. Kirschbaum, I. A. Goodman, G. M. O'Donnell, and D. P. Lettenmaier, 2000: Effects of land cover change on streamflow in the interior Columbia River basin (USA and Canada). *Hydrol. Processes,* **14,** 867–885.

Maurer, E. P., A. W. Wood, J. C. Adam, D. P. Lettenmaier, and B. Nijssen, 2002: A long-term hydrologically based dataset of land surface fluxes and states for the conterminous United States. *J. Climate,* **15,** 3237–3251.

Mitchell, K. E., and Coauthors, 2004: The multi-institution North American Land Data Assimilation System (NLDAS): Utilizing multiple GCIP products and partners in a continental distributed hydrological modeling system. *J. Geophys. Res.,* **109,** D07S90, doi:10.1029/2003JD003823.

Nijssen, B., R. Schnur, and D. P. Lettenmaier, 2001: Global retrospective estimation of soil moisture using the Variable Infiltration Capacity land surface model, 1980–93. *J. Climate,* **14,** 1790–1808.

Niu, G.-Y., Z.-L. Yang, R. E. Dickinson, and L. E. Gulden, 2005: A simple TOPMODEL-based runoff parameterization (SIMTOP) for use in global climate models. *J. Geophys. Res.,* **110,** D21106, doi:10.1029/2005JD006111.

——, ——, ——, ——, and H. Su, 2007: Development of a simple groundwater model for use in climate models and evaluation with Gravity Recovery and Climate Experiment data. *J. Geophys. Res.,* **112,** D07103, doi:10.1029/2006JD007522.

Oleson, K. W., G. B. Bonan, S. Levis, and M. Vertenstein, 2004: Effects of land use change on North American climates: Impact of surface datasets and model biogeophysics. *Climate Dyn.,* **23,** 117–132.

——, and Coauthors, 2007: CLM 3.5 documentation. UCAR, 34 pp. [Available online at http://www.cgd.ucar.edu/tss/clm/distribution/clm3.5/CLM3_5_documentation.pdf.]

Palmer, W. C., 1965: Meteorological drought. U.S. Department of Commerce Weather Bureau Research Paper 45, 58 pp.

Ross, T., and N. Lott, 2003: A climatology of 1980-2003 extreme weather and climate events. National Climatic Data Center Tech. Rep. 2003-01, 14 pp.

Schaake, J. C., V. I. Koren, Q.-Y. Duan, K. E. Mitchell, and F. Chen, 1996: Simple water balance model for estimating runoff at different spatial and temporal scales. *J. Geophys. Res.,* **101,** 7461–7475.

Schubert, S. D., M. J. Suarez, P. J. Region, R. D. Koster, and J. T. Bacmeister, 2004a: Causes of long-term drought in the U.S. Great Plains. *J. Climate,* **17,** 485–503.

——, ——, ——, ——, and ——, 2004b: On the cause of the 1930s Dust Bowl. *Science,* **303,** 1855–1859.

Svoboda, M., and Coauthors, 2002: The drought monitor. *Bull. Amer. Meteor. Soc.,* **83,** 1183–1190.

Tang, Q., A. W. Wood, and D. P. Lettenmaier, 2009: Real-time precipitation estimation based on index station percentiles. *J. Hydrometeor.,* **10,** 266–277.

Trenberth, K., 2004: Exploring drought and its implications for the future. *Eos, Trans. Amer. Geophys. Union,* **85,** doi:10.1029/2004EO030004.

——, and Coauthors, 2007: Observations: Surface and atmospheric climate change. *Climate Change 2007: The Physical Science Basis,* S. Solomon et al., Eds., Cambridge University Press, 235–336.

Wang, A., X. Zeng, S. S. P. Shen, Q.-C. Zeng, and R. E. Dickinson, 2006: Time scales of land surface hydrology. *J. Hydrometeor.,* **7,** 868–879.

——, K. Y. Li, and D. P. Lettenmaier, 2008: Integration of variable infiltration capacity model soil hydrology scheme into the community land model. *J. Geophys. Res.,* **113,** D09111, doi:10.1029/2007JD009246.

Wilhite, D. A., 1983: Government response to drought in the United States: With particular reference to the Great Plains. *J. Climate Appl. Meteor.,* **22,** 40–50.

Wood, A. W., 2008: The University of Washington Surface Water Monitor: An experimental platform for national hydrologic assessment and prediction. Preprints, *22nd Conf. on Hydrology,* New Orleans, LA, Amer. Meteor. Soc., 5.2. [Available online at http://ams.confex.com/ams/pdfpapers/134844.pdf.]

——, and D. P. Lettenmaier, 2006: Test bed for new seasonal hydrologic forecasting approaches in the western United States. *Bull. Amer. Meteor. Soc.,* **87,** 1699–1712.

——, and Coauthors, 1998: The Project for Intercomparison of Land-surface Parameterization Schemes (PILPS) phase 2(c) Red–Arkansas River basin experiment: 1. Experiment description and summary intercomparisons. *Global Planet. Change,* **19,** 115–135.

Woodhouse, C. A., and J. T. Overpeck, 1998: 2000 years of drought variability in the central United States. *Bull. Amer. Meteor. Soc.,* **79,** 2693–2714.

World Meteorological Organization, 1969: Manual for depth-area-duration analysis of storm precipitation. WMO Rep. 237.TP.129, 114 pp.